



Light- and microwave-induced spin current and spin-to-charge conversion in magnetic quantum material heterostructures

M. Benjamin Jungfleisch

Department of Physics and Astronomy, University of Delaware, Newark, DE 19716, USA



UNIVERSITY OF DELAWARE

CENTER FOR HYBRID, ACTIVE,
AND RESPONSIVE MATERIALS



October 11, 2023



Team and Collaborators



University of Delaware

Weipeng Wu

Duy Quang To

Anderson Janotti

Lars Gundlach

Morgan State University

Vinay Sharma

Prabesh Bajracharya

Anthony Johnson

Ramesh C. Budhani

NIST

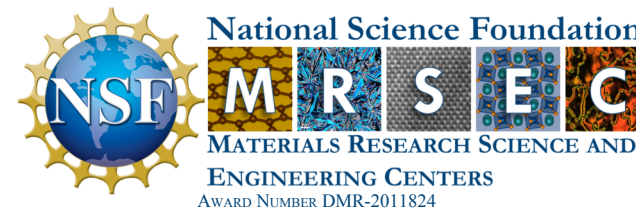
Garnett W. Bryant

Argonne National Labs

Haidan Wen

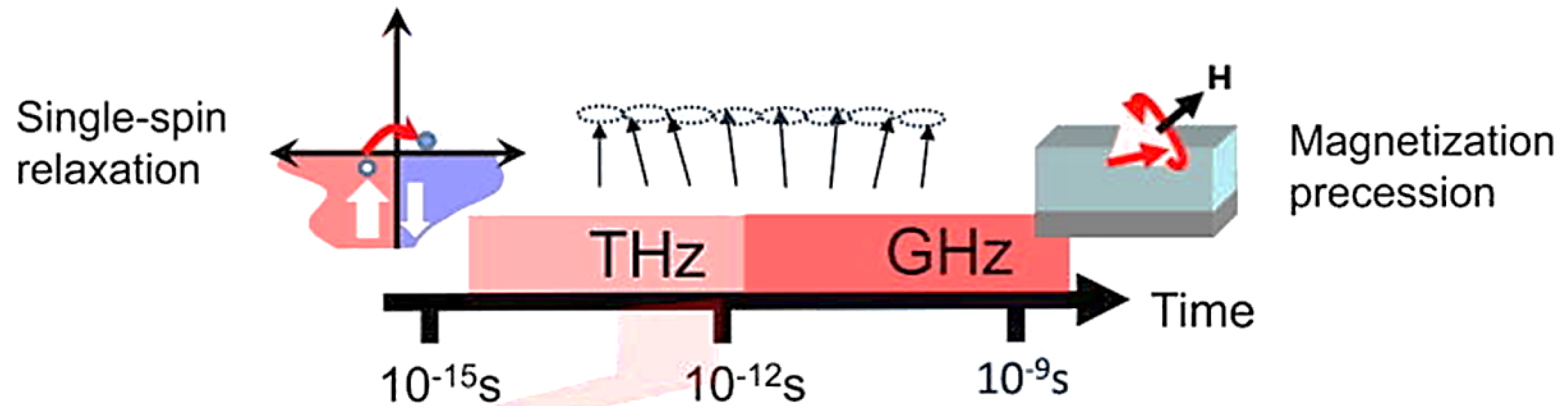
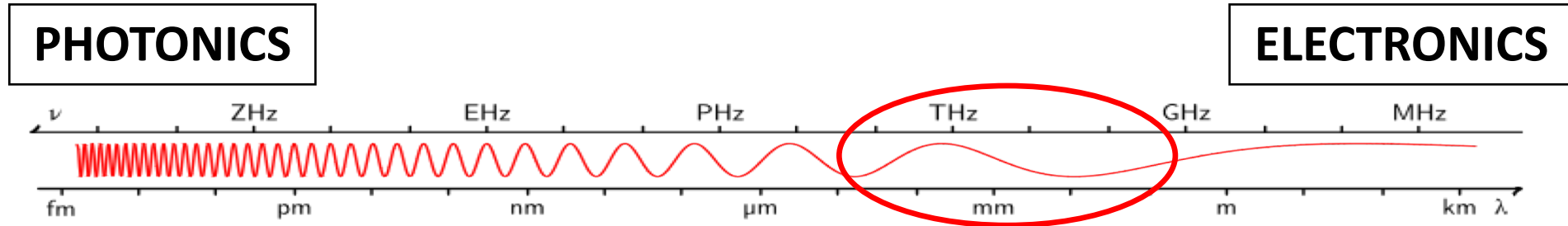
Richard D. Schaller

Acknowledgment

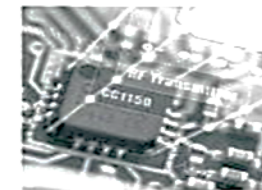
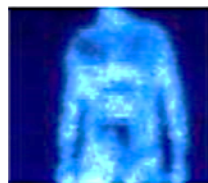


Additional support received by NSF under Grant No. 1833000 and the University of Delaware Research Foundation

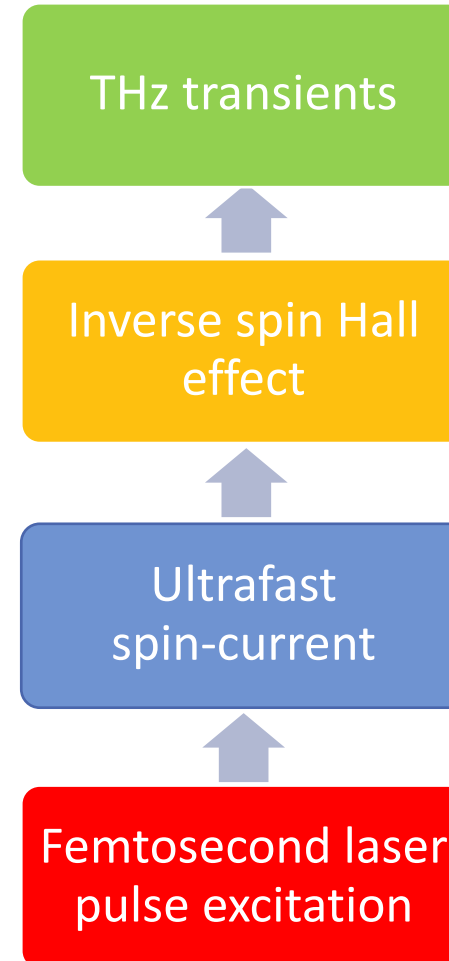
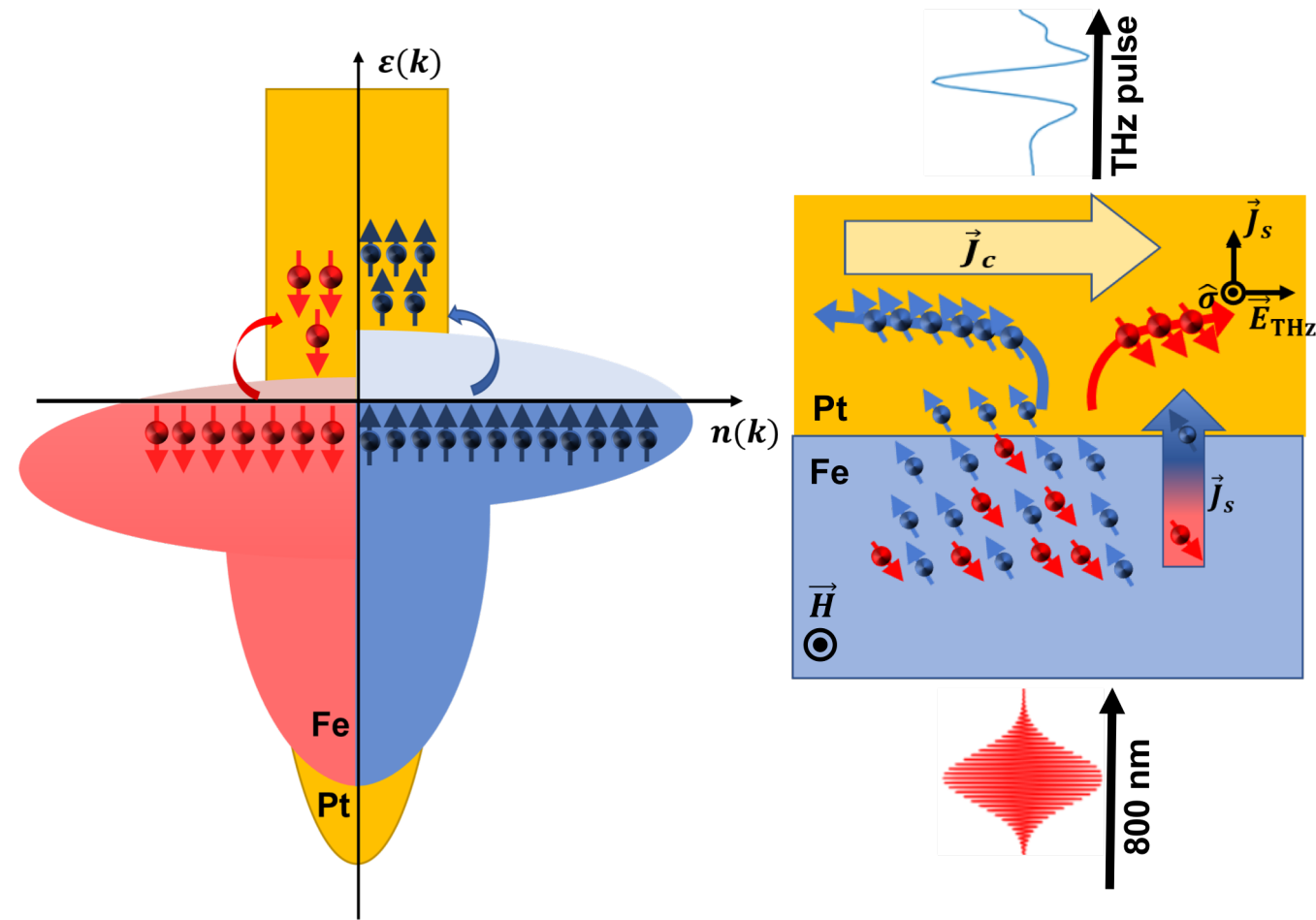
Terahertz technologies



Applications: security, bio scanner, pharmaceuticals and food control, mobile phone, inter-chip wireless, data bit addressing and transfer



Spintronic terahertz emitter

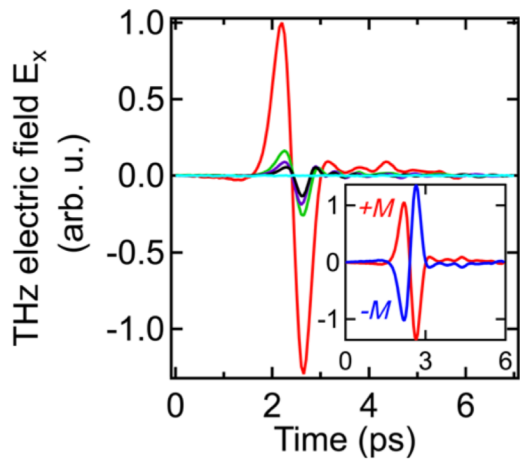
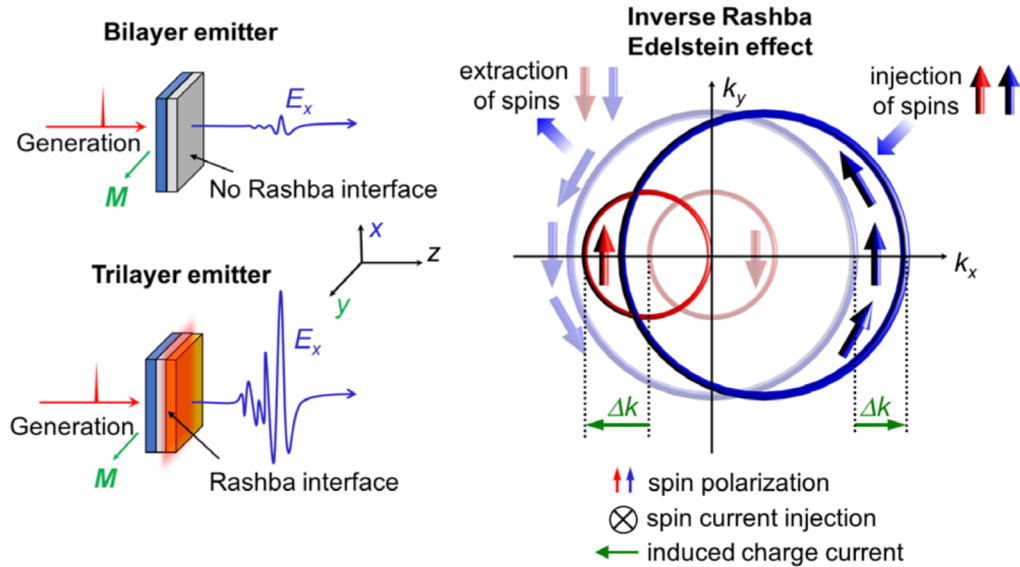


- High signal strength
- Broadband
- Inexpensive and easy to fabricate

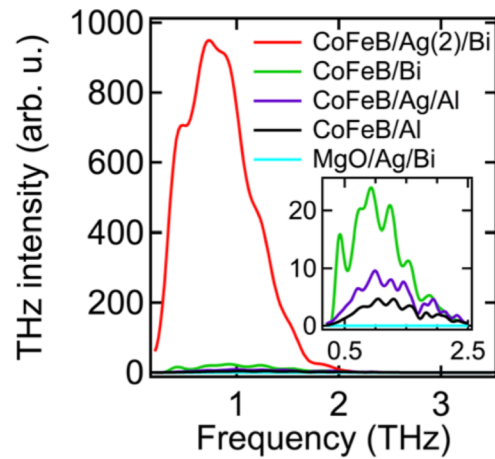
Inverse spin Hall effect: $\vec{J}_c \propto \theta_{SH} \vec{J}_s \times \vec{\sigma}$

Wu, ..., MBJ et al., J. Appl. Phys. **130**, 091101 (2021)

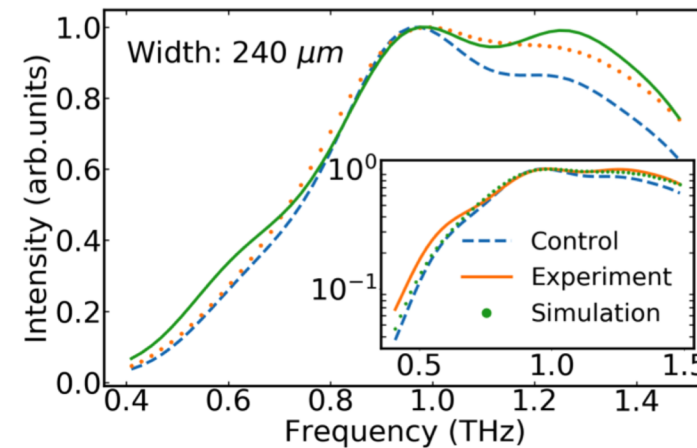
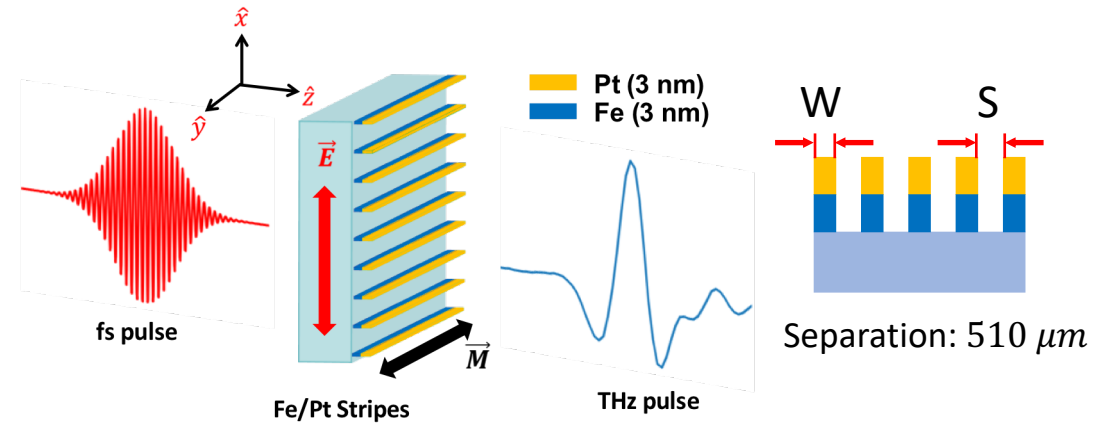
Control of THz emission by spin-charge current conversion at Rashba interfaces



MBJ et al., Phys. Rev. Lett. **120**, 207207 (2018)

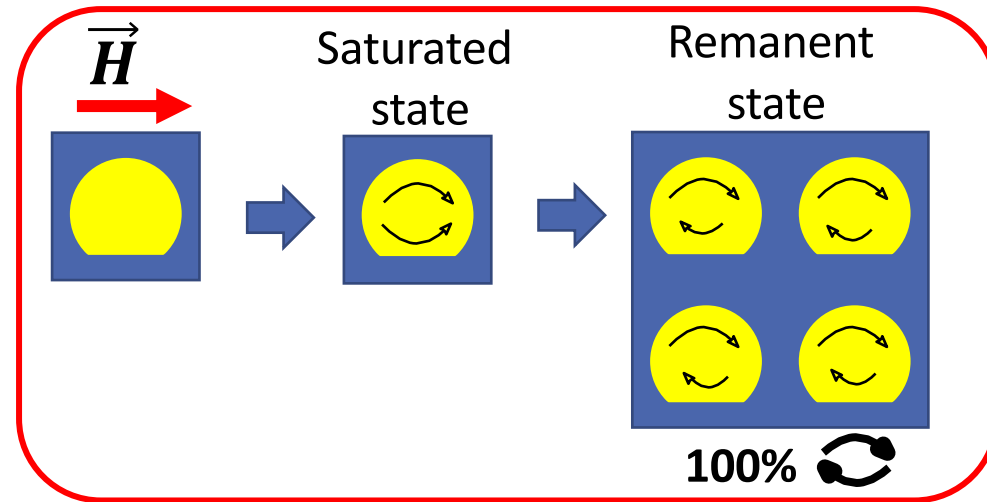


Modification of THz emission using microfabricated spintronic emitters

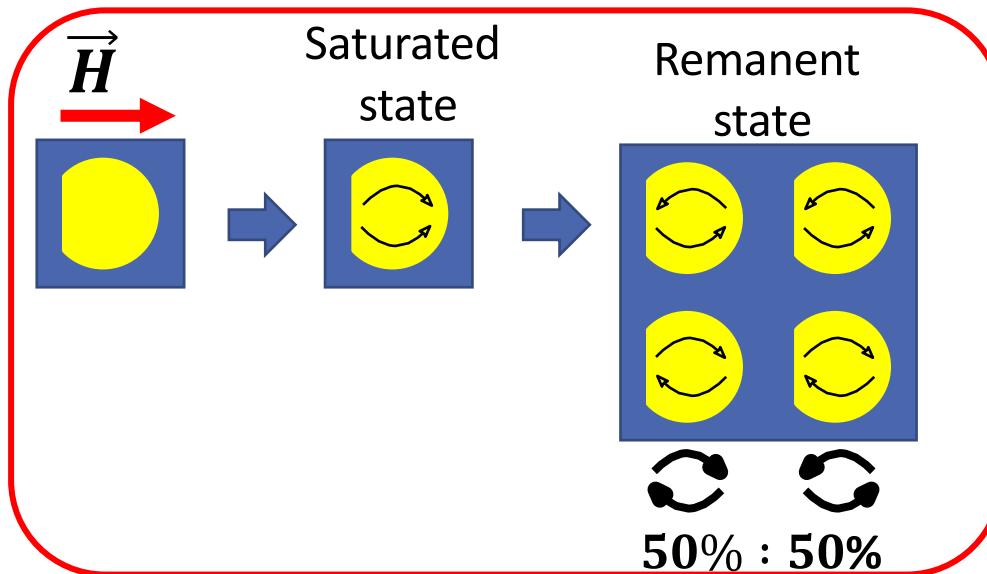


Wu, ..., MBJ et al., J. Appl. Phys. **128**, 103902 (2020)

Controlling polarization by remanent magnetization - concept



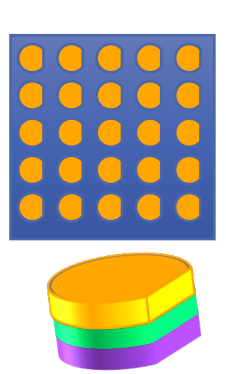
Same
chirality



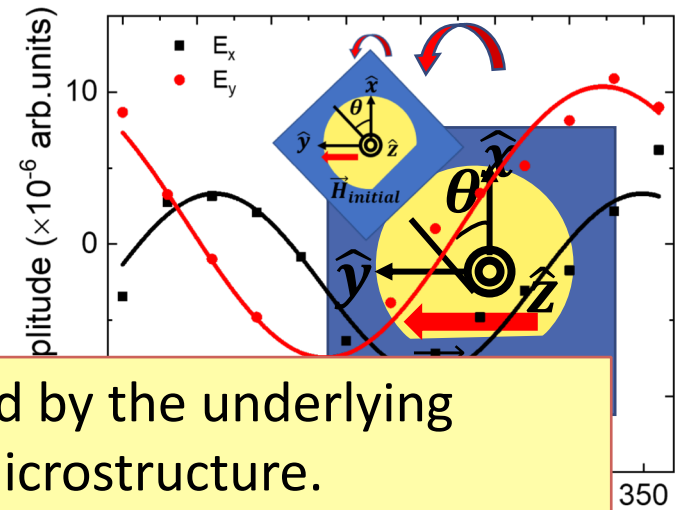
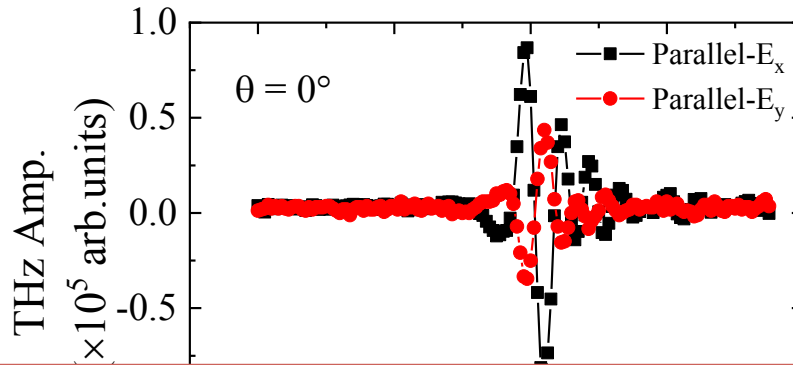
Random
chirality

Wu, ..., MBJ et al., Appl. Phys. Lett. **121**, 052401 (2022)

Controlling polarization by remanent magnetization - realization

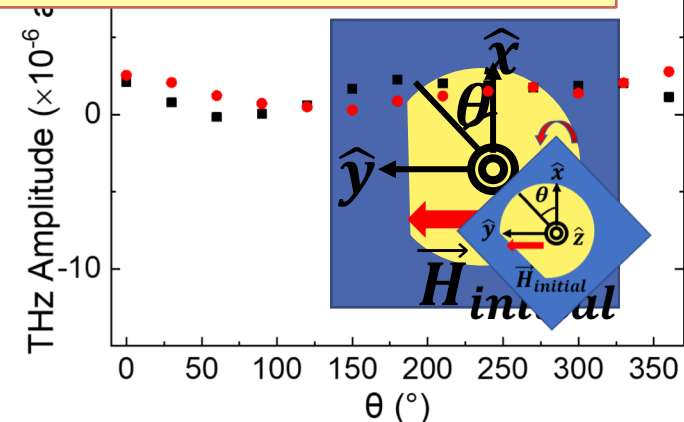
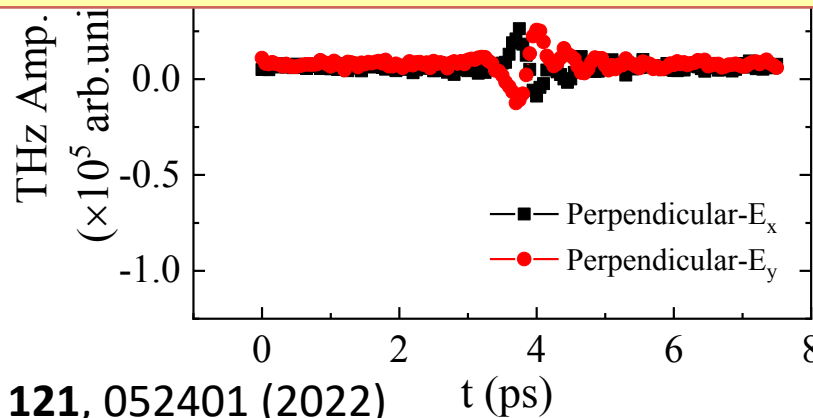


2 μm
5 μm



- Precise tunability of the polarization state is facilitated by the underlying magnetization texture dictated by the shape of the microstructure.
- These results reveal the underlying physical mechanisms of a nonuniform magnetization state on the generation of ultrafast spin currents.

5 nm
Sapphire

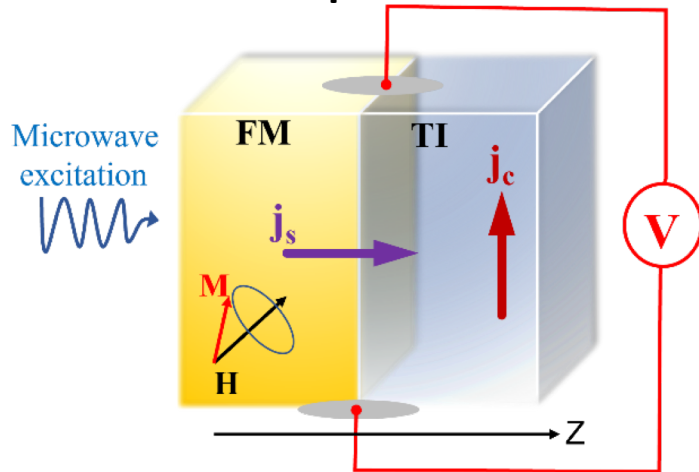


Wu, ..., MBJ et al., Appl. Phys. Lett. **121**, 052401 (2022)

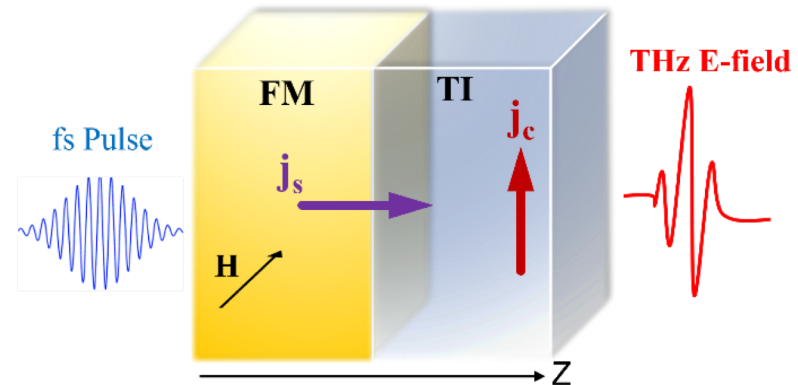
Outline: Spin current injection across FM/ TI interfaces



GHz inverse spin Hall effect experiment



THz emission inverse spin Hall effect experiment



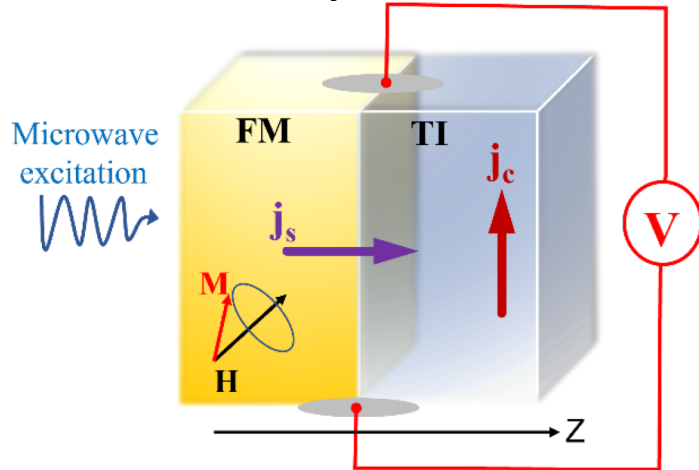
Ferromagnet/ 3D topological insulator heterostructures grown by DC magnetron sputtering:

- Sapphire(substrate)//Fe₇₈Ga₁₃B₉(**FeGaB**)/Bi₈₅Sb₁₅(**BiSb**)/MgO(capping)
 - Amorphous FeGaB → [Phys. Rev. Materials 5, 124410 \(2021\)](#)
 - BiSb with (001) texture
- MgAl₂O₄(substrate)// Fe₇₅Co₂₅(**FeCo**) / Bi₂Te₃(**BiTe**)/Al(capping)
 - Epitaxial FeCo with body-centered cubic (bcc) structure
 - Polycrystalline BiTe → [Appl. Phys. Lett. 122, 072403 \(2023\)](#)

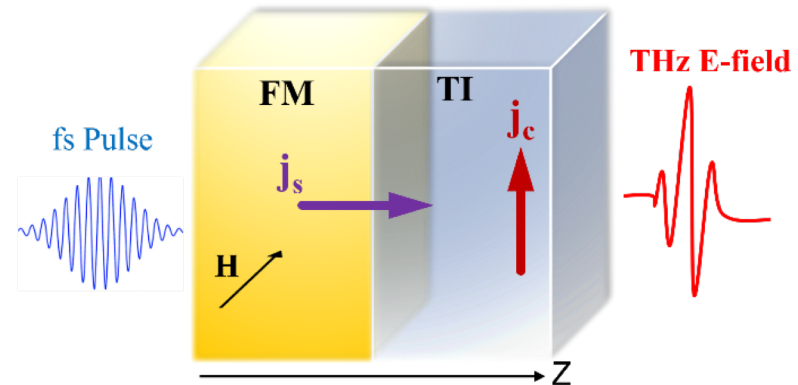
Outline: Spin current injection across FM/ TI interfaces



GHz inverse spin Hall effect experiment



THz emission inverse spin Hall effect experiment



Ferromagnet/ 3D topological insulator heterostructures grown by DC magnetron sputtering:

- **Sapphire(substrate)//Fe₇₈Ga₁₃B₉(FeGaB)/Bi₈₅Sb₁₅(BiSb)/MgO(capping)**
 - Amorphous FeGaB
 - BiSb with (001) texture
- MgAl₂O₄(substrate)// Fe₇₅Co₂₅(FeCo) / Bi₂Te₃(BiTe)/Al(capping)
 - Epitaxial FeCo with body-centered cubic (bcc) structure
 - Polycrystalline BiTe

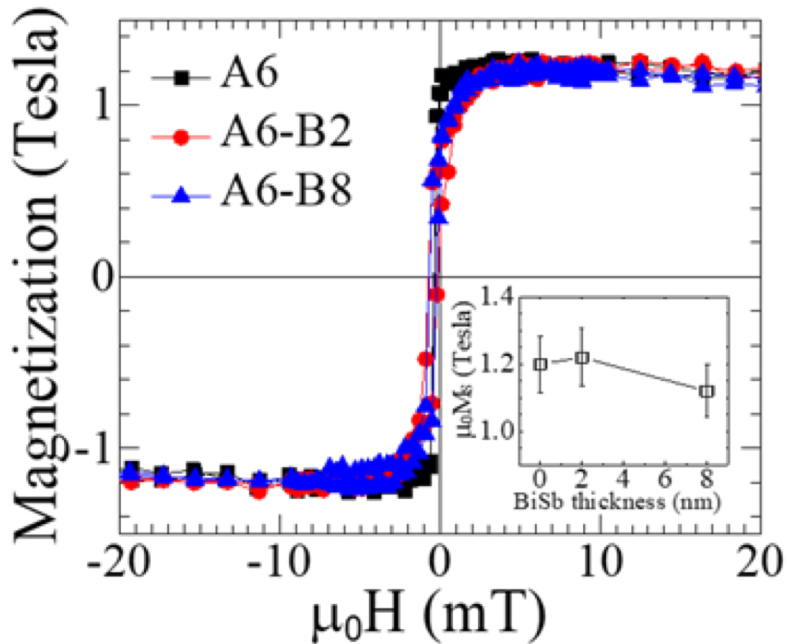
Bilayer thin film growth and characterization



DC magnetron sputtering: **Fe₇₈Ga₁₃B₉** and **Bi₈₅Sb₁₅**

Thickness FeGaB: 6 nm, BiSb: 0, 1, 2, 4, 6, 8, 10, 15, 20 nm

We refer FeGaB(6)/BiSb(2) as A6-B2.



- Similar saturation magnetization M_s of 1.2 ± 0.14 T for bilayer with different thickness of BiSb
- Small coercivity field of $\mu_0 H \leq 2$ mT indicating a soft magnetic character of the FeGaB films with in-plane magnetization



The deposition of BiSb on top of FeGaB does not affect the magnetization significantly

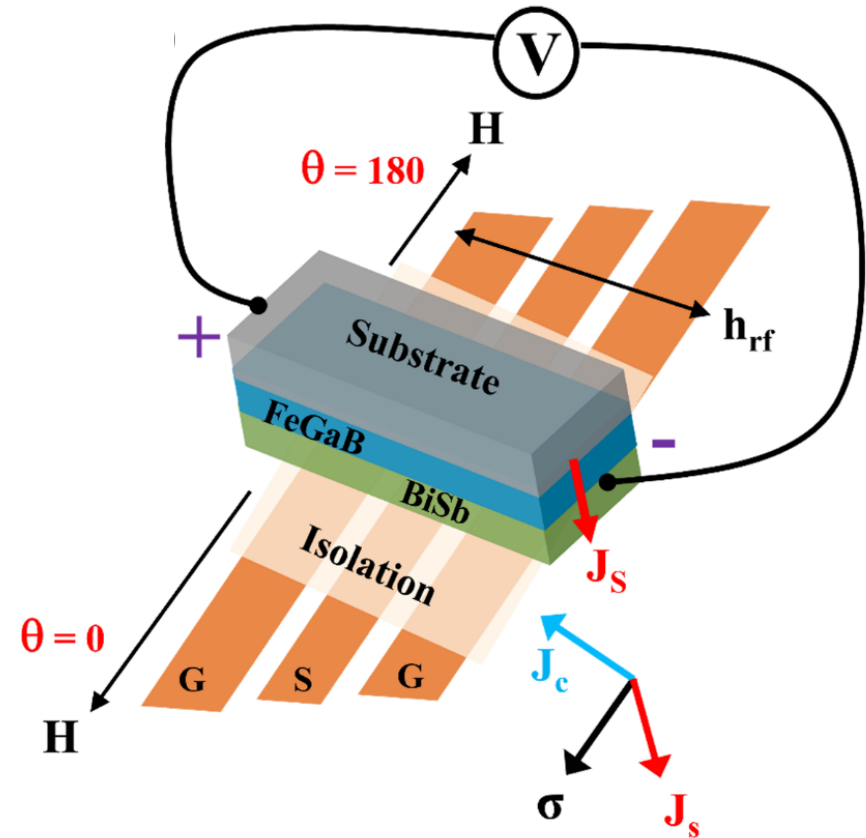
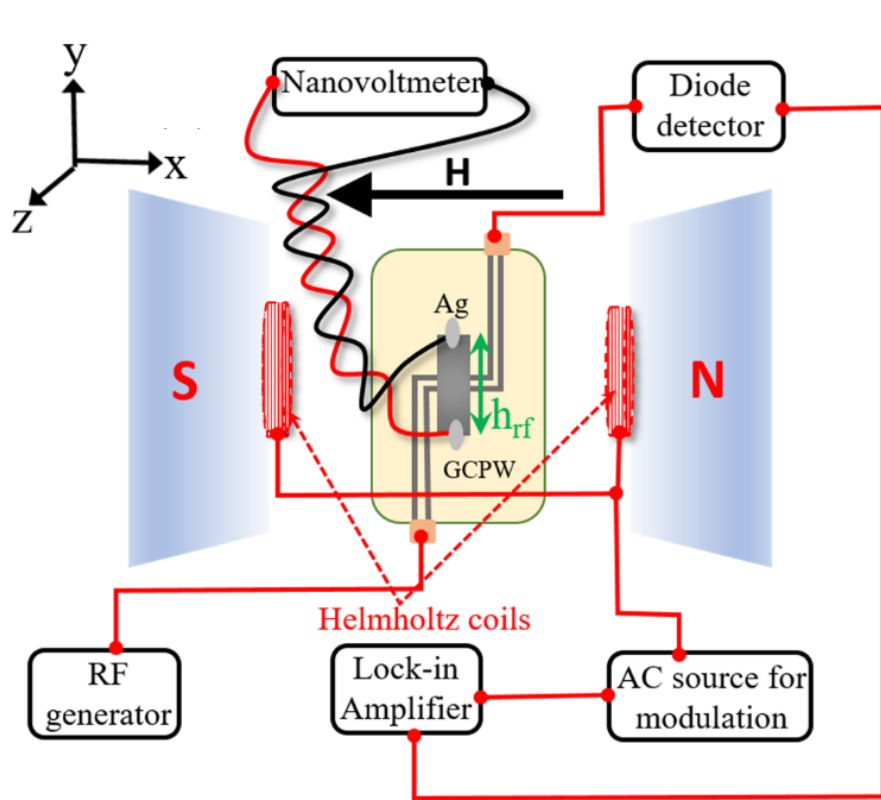
Sharma, Wu, ..., MBJ et al., Phys. Rev. Materials **5**, 124410 (2021)

Experimental setup for combined FMR/ISHE



Ferromagnetic resonance (FMR): Gilbert damping $\alpha \rightarrow$ spin-mixing conductance $g^{\downarrow\uparrow}$

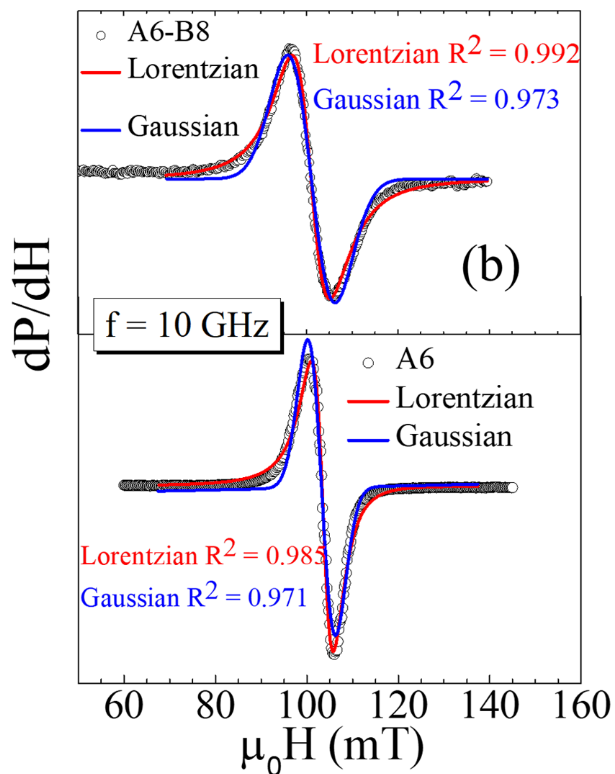
Inverse spin-Hall effect (ISHE): spin-to-charge current conversion \rightarrow spin-Hall angle θ_{SH} and spin-diffusion length λ_{SD} of BiSb



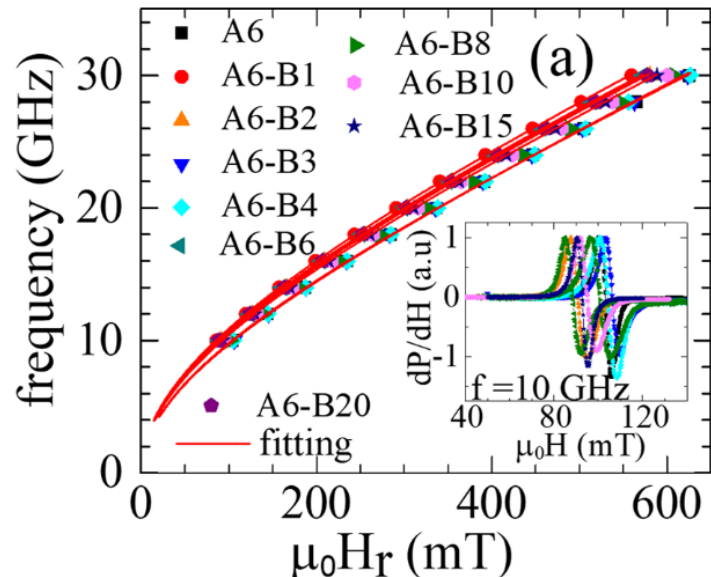
Sharma, Wu, ..., MBJ et al., Phys. Rev. Materials **5**, 124410 (2021)

Ferromagnetic resonance (FMR)

Differential absorption



High degree of magnetic homogeneity of FeGaB film



$H_r, \Delta H$

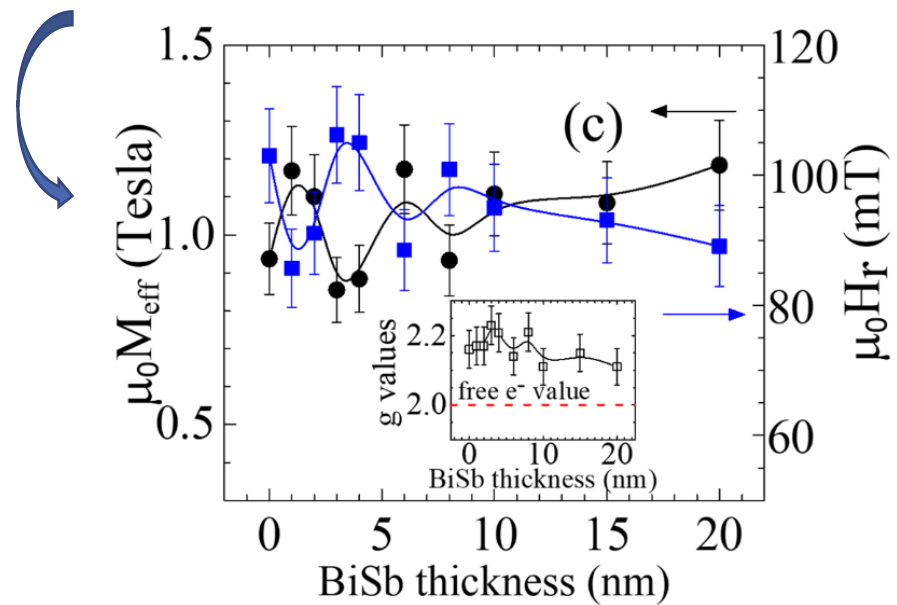
$$\frac{dP}{dH} = K_1 \frac{4\Delta H(H - H_r)}{[4(H - H_r)^2 + (\Delta H)^2]^2} - K_2 \frac{(\Delta H)^2 - 4(H - H_r)^2}{[4(H - H_r)^2 + (\Delta H)^2]^2}$$

K_1, K_2 : symmetric & antisymmetric Lorentzian coefficients

$$f = \frac{\gamma}{2\pi} \mu_0 \sqrt{H(H + M_{eff})}$$

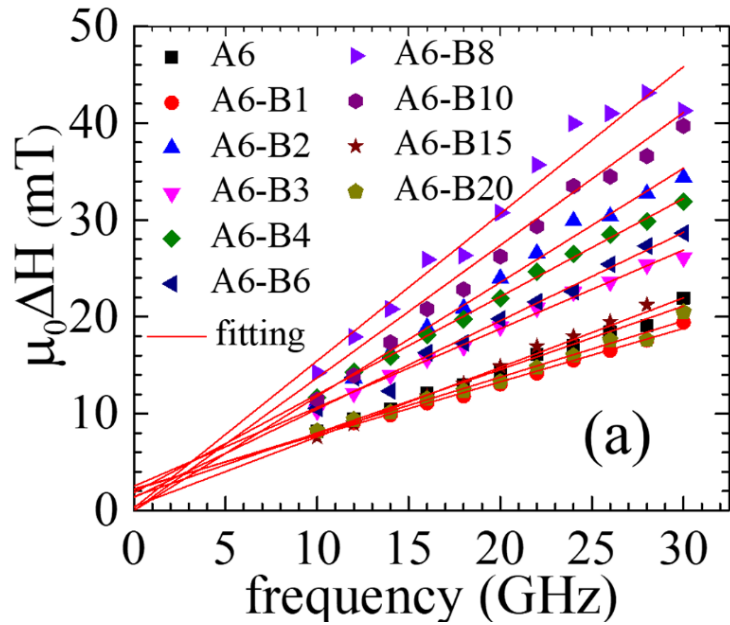
$$\gamma = \frac{g\mu_B}{h} \text{ and } \mu_0 M_{eff} = \mu_0(M_s - H_s)$$

M_{eff} , Landé g-factor fitting parameters

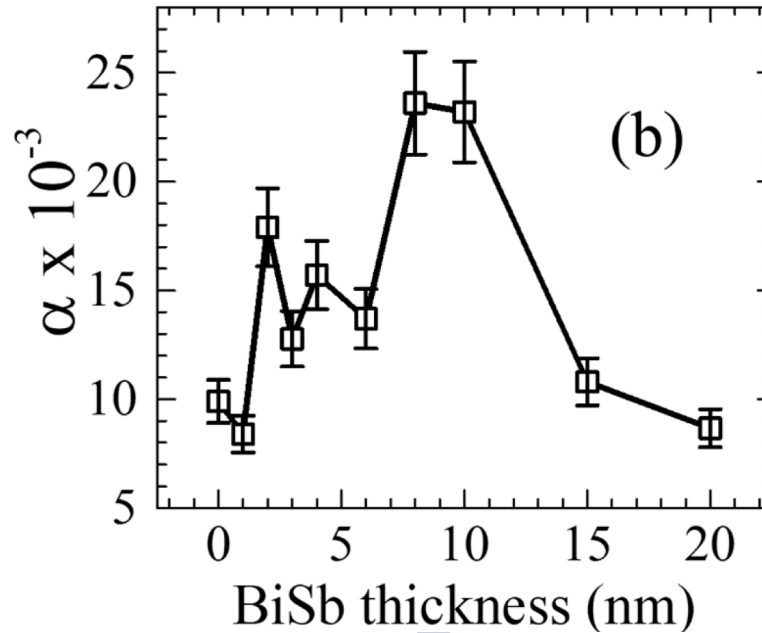


Small variation of $\mu_0 M_{eff}$ and $\mu_0 M_s$ suggests metallurgically clean interface with FeGaB layer

BiSb-thickness dependent variation of Gilbert damping



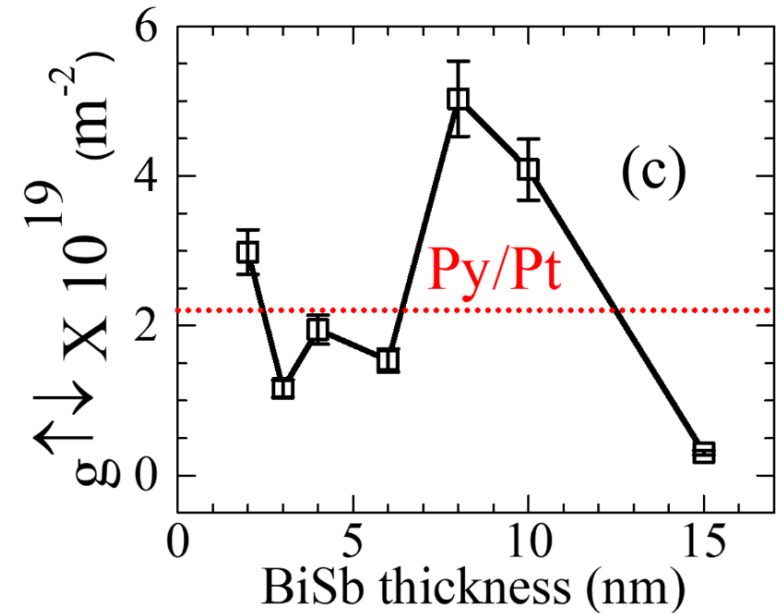
$$\Delta H = \Delta H_0 + \frac{4\pi\alpha}{\gamma} f$$



- FMR linewidth is enhanced in FeGaB/BiSb bilayer
- The rapid increase of α indicates efficient absorption of spin current in BiSb layer

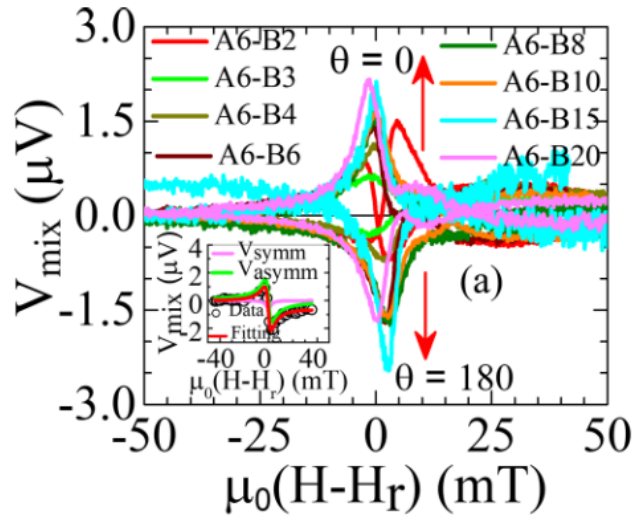
Spin mixing conductance $g^{\uparrow\downarrow}$:

$$g^{\uparrow\downarrow} = \frac{4\pi M_s t_{FeGaB}}{g\mu_B} (\alpha_{FeGaB-BiSb} - \alpha_{FeGaB})$$



Topological surface state plays an important role!

Inverse spin Hall effect (ISHE) of BiSb



$$V_{mix} = K_s \frac{\delta H^2}{(H - H_r)^2 + \delta H^2} + K_{as} \frac{-2\delta H(H - H_r)}{(H - H_r)^2 + \delta H^2}$$

V_{symm}:

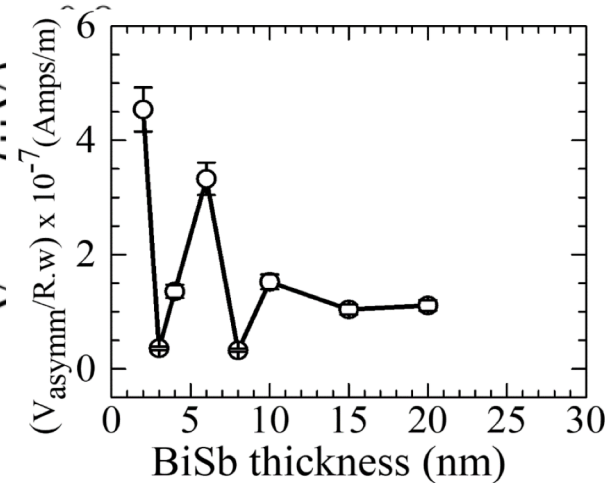
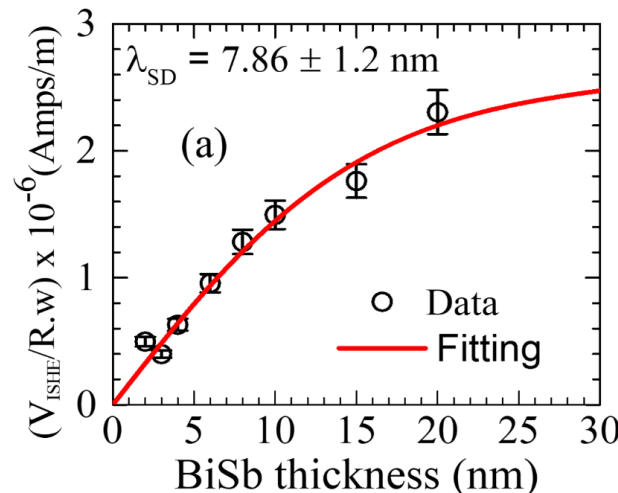
- Spin-pumping induced ISHE in BiSb
- Self-induced ISHE in FeGaB

V_{asymm}:

- Anisotropic magnetoresistance
- Anomalous Hall effect

- Positive spin Hall angle of BiSb
- Opposite spin Hall angle for bare FeGaB compared to FeGaB/BiSb

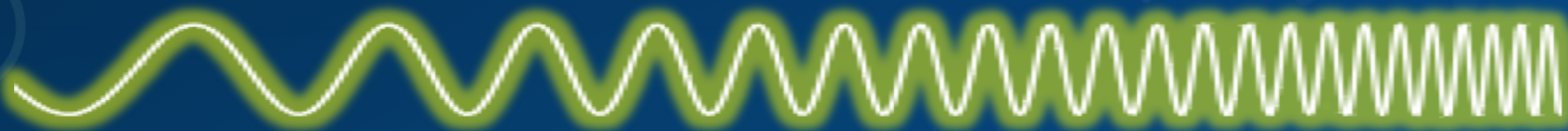
BiSb(8 nm): $\theta_{SH} = 0.007 \pm 0.001$
BiSb(10 nm): $\theta_{SH} = 0.010 \pm 0.001$



Damped-oscillator-like behavior due to opposite signs of AMR in FeGaB and BiSb

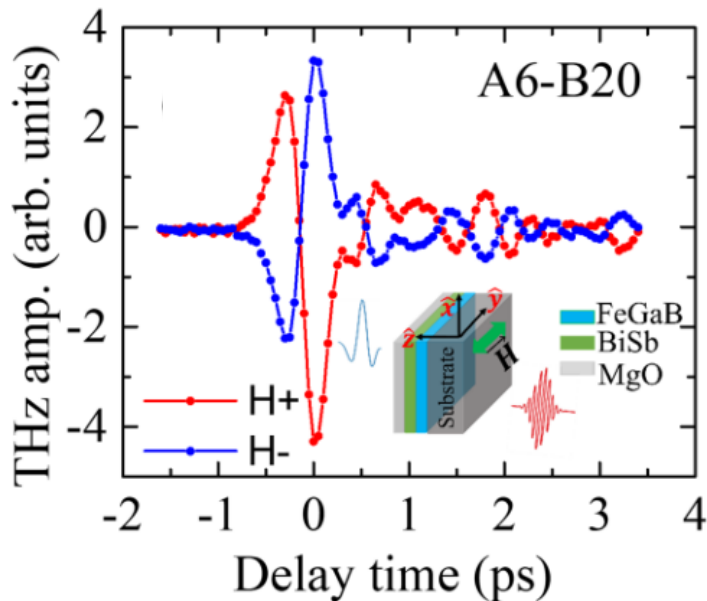
How do GHz dynamics translate to the THz range?

GHz



THz

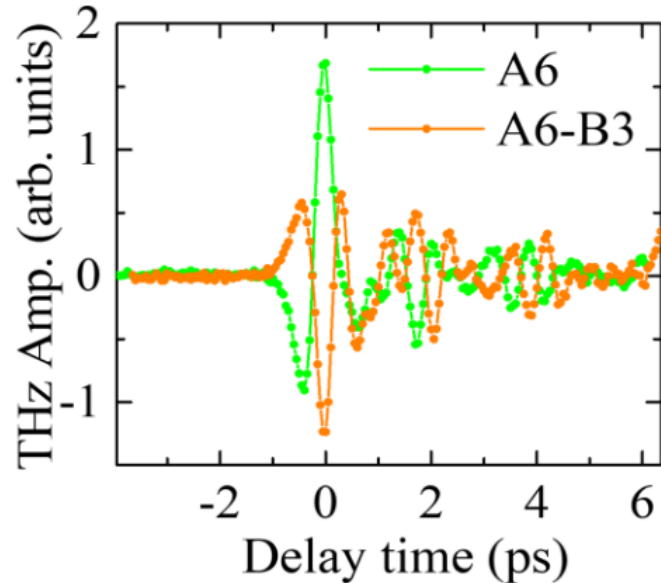
THz emission experiments



Signal inverted when reversing the magnetic field



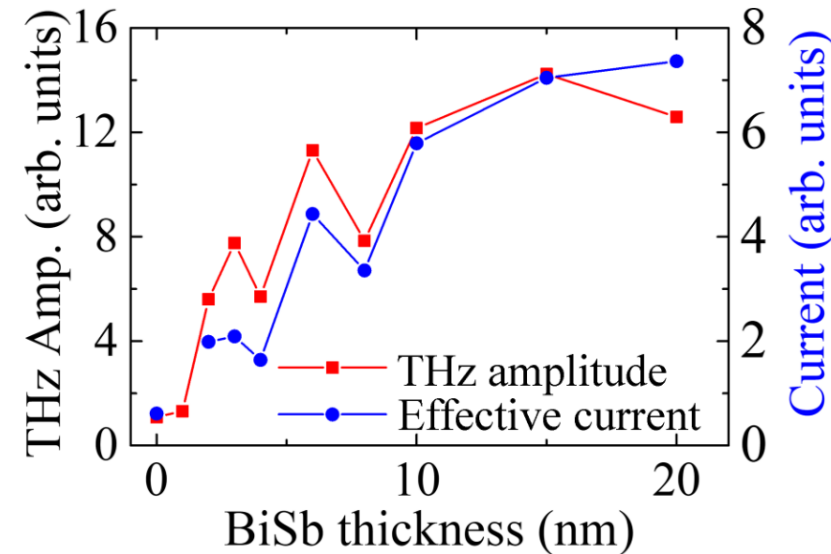
Magnetic origin of the THz emission



Opposite sign of bare FeGaB and FeGaB/BiSb bilayer



SHA θ_{SH} of FeGaB and FeGaB/BiSb opposite

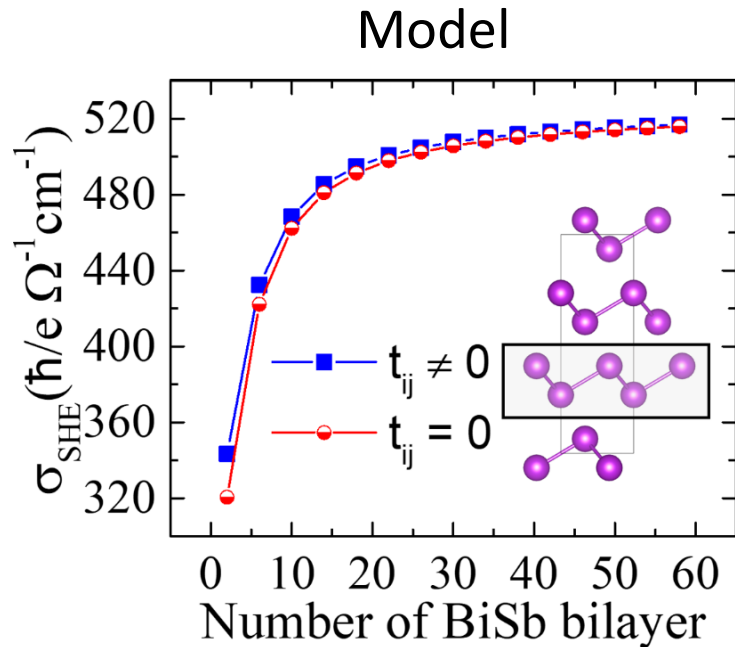


Effective current:

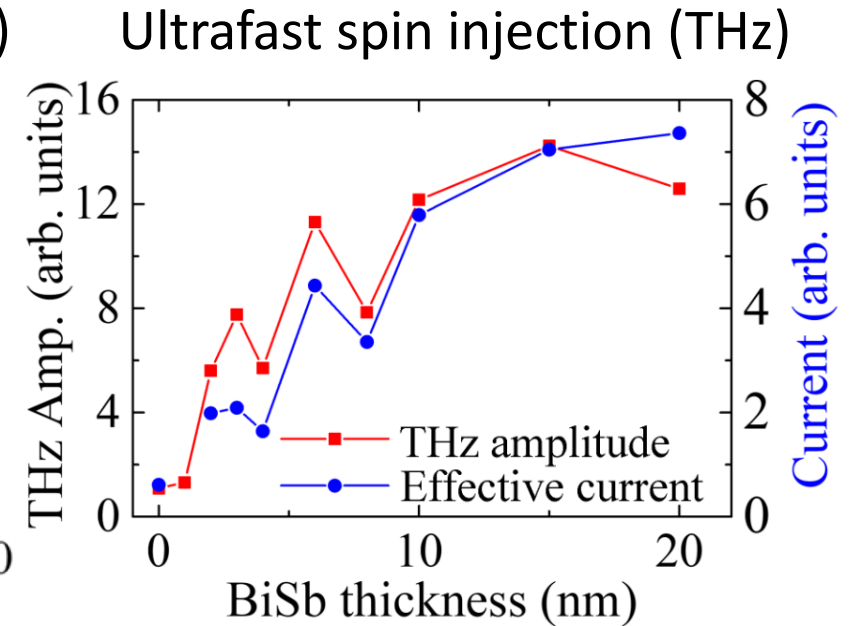
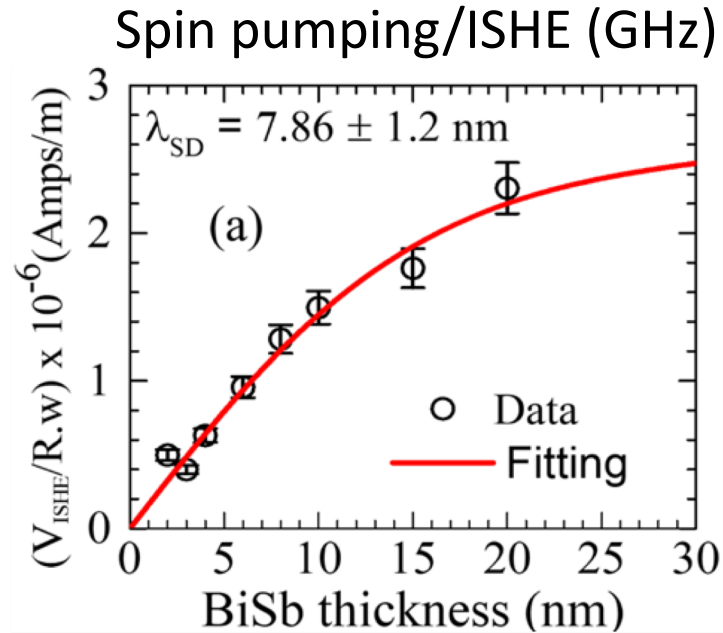
$$I_{eff} = \frac{E_{THz}}{R}$$
 R: DC resistance of bilayer

Experimental results of light and microwave driven spin pumping across FeGaB–BiSb interface in agreement.

Comparison to theory: Tight-binding model of BiSb



$t_{ij} \neq 0$ and $t_{ij} = 0$ correspond to the case with and without surface Rashba effect



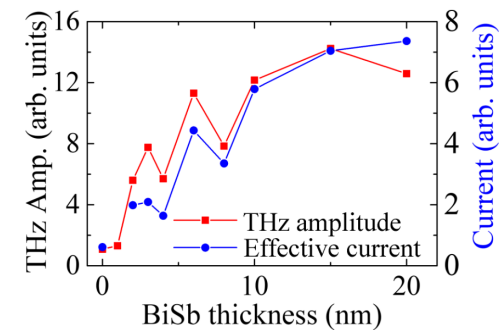
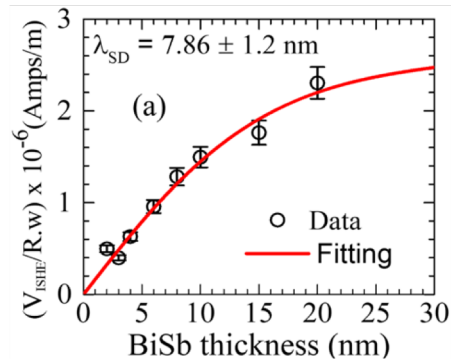
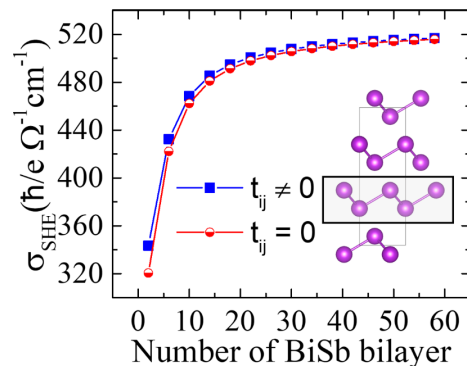
Increased BiSb thickness leads to an increase of spin-Hall conductivity σ_{SHE} , hence increasing the spin-to-charge conversion efficiency in GHz and THz experiments.

Modeling by To, Janotti, Bryant (UDCHARM)

Take-home messages - Part 1

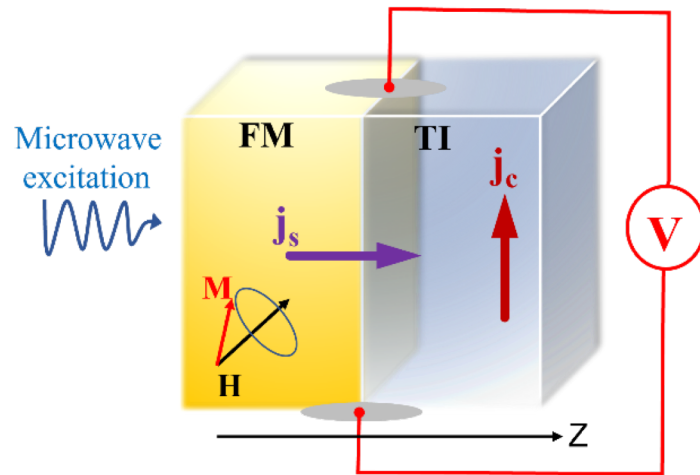


- Metallurgically clean interface between FeGaB and BiSb layer
- Unconventional thickness dependence of $g^{\downarrow\uparrow}$ in FeGaB/BiSb
- Spin-pumping-induced DC measurements enable separation of contributions from AMR and ISHE
- Spin Hall angle ($\theta_{SH} = 0.010$) and spin-diffusion length ($\lambda_{SD} = 7.86 \text{ nm}$) of BiSb determined
- Agreement between GHz, THz experiments & linear response theory based on Kubo-Bastin formula considering a tight-binding model

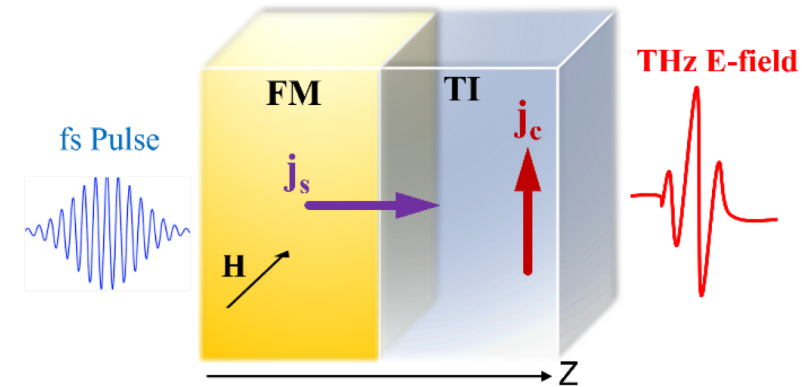


Outline: Spin current injection across FM/ TI interfaces

GHz inverse spin Hall experiment



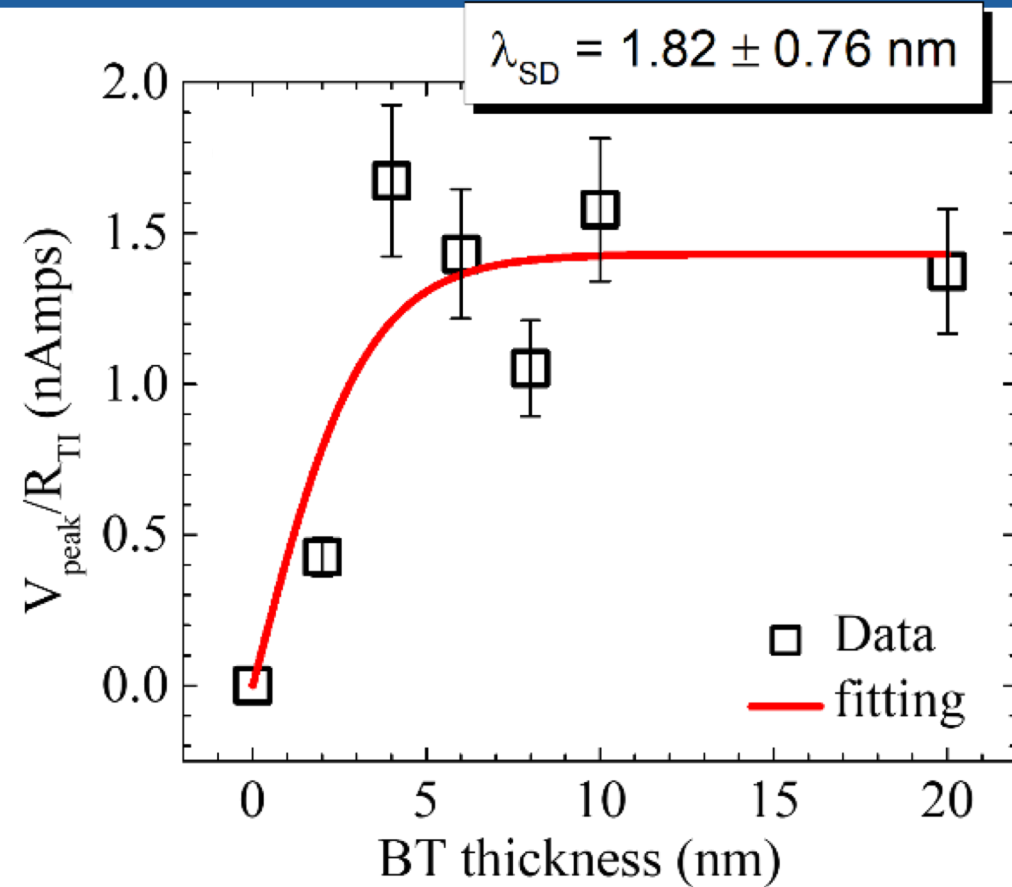
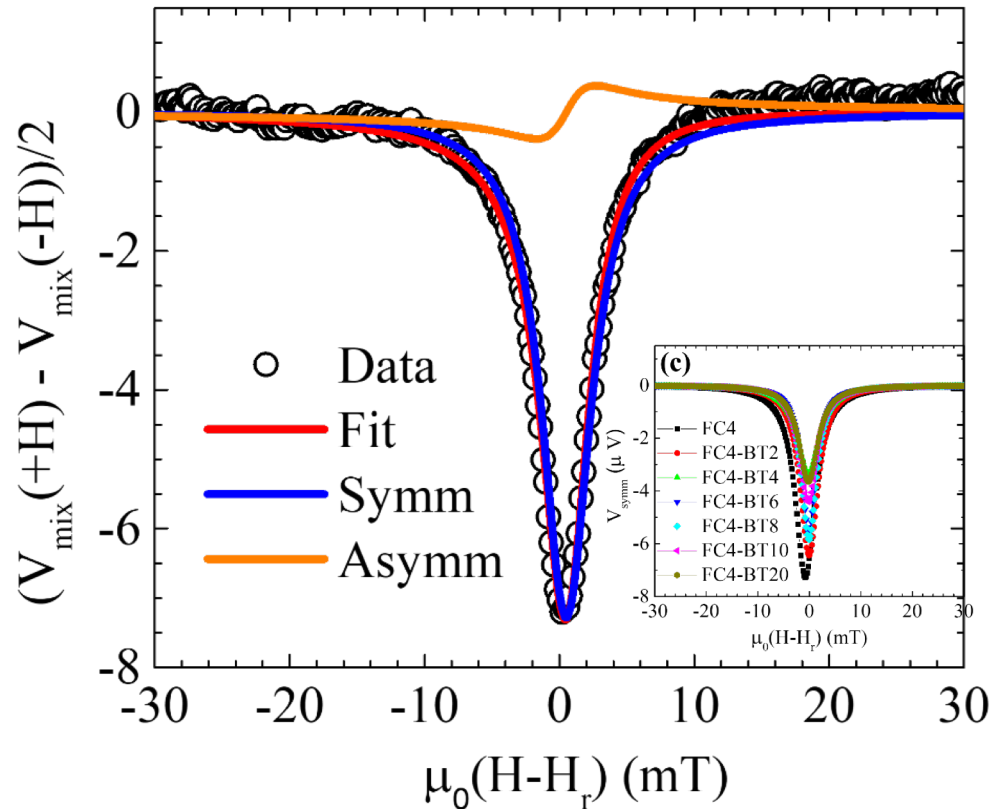
THz emission mediated by inverse spin Hall experiment



Materials of interest (ferromagnet/3D topological insulator) grown by DC magnetron sputtering:

- Sapphire(substrate)//Fe₇₈Ga₁₃B₉(FeGaB)/Bi₈₅Sb₁₅(BiSb)/MgO(capping)
 - Amorphous FeGaB
 - BiSb with (001) texture
- **MgAl₂O₄(substrate)// Fe₇₅Co₂₅(FeCo) / Bi₂Te₃(BiTe)/Al(capping)**
 - **Epitaxial FeCo with body-centered cubic (bcc) structure**
 - **Polycrystalline BiTe**

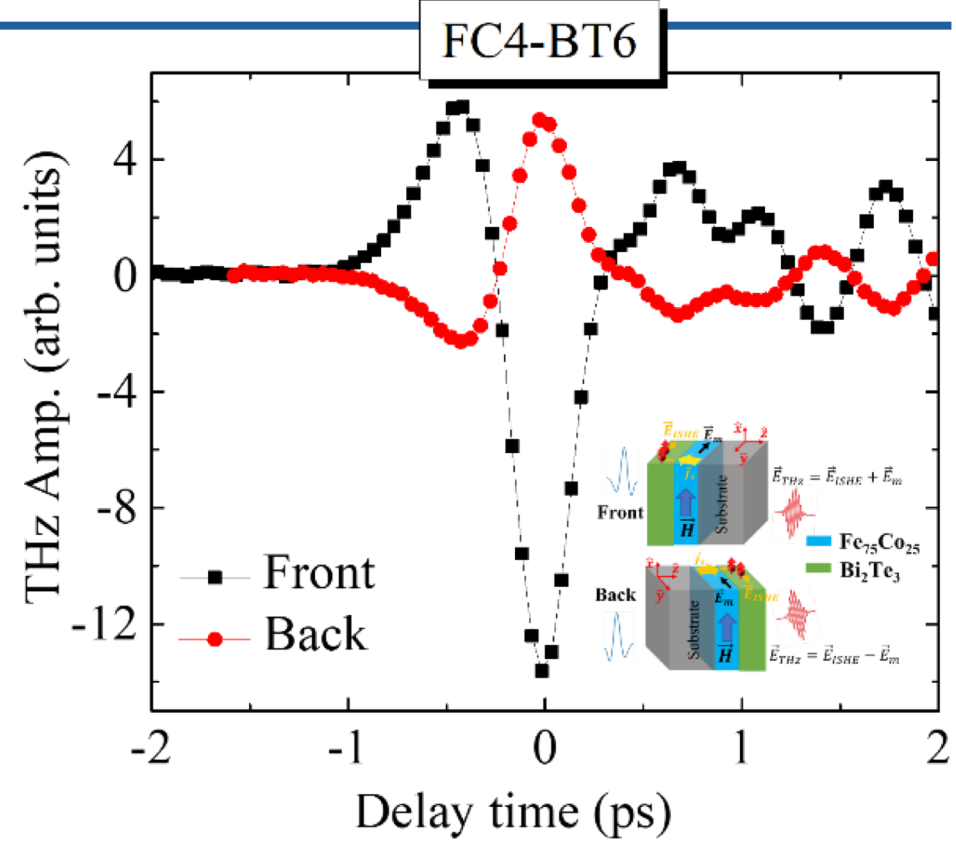
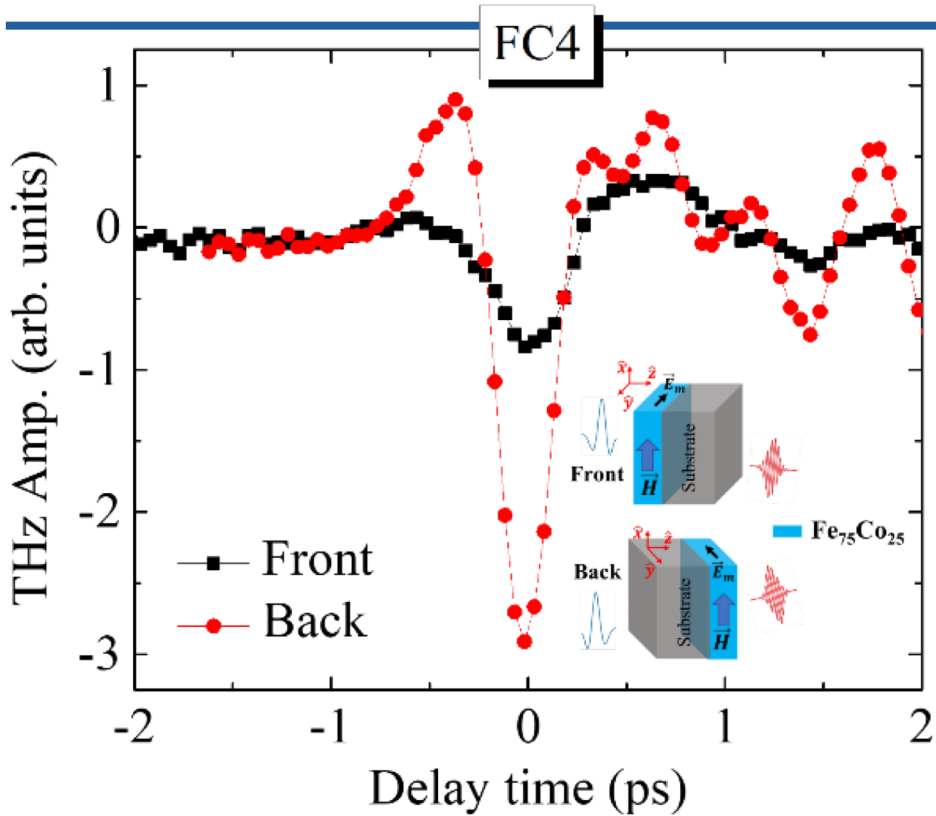
GHz – ISHE studies: FeCo/BiTe



$$V_{mix} = K_s \frac{H^2}{(H - H_r)^2 + H^2} + K_{as} \frac{-2H(H - H_r)}{(H - H_r)^2 + H^2}$$

ISHE and rectification effects

THz – ISHE studies: FeCo/BiTe



Magnetic dipole radiation



AMR/AHE +
self-induced-ISHE

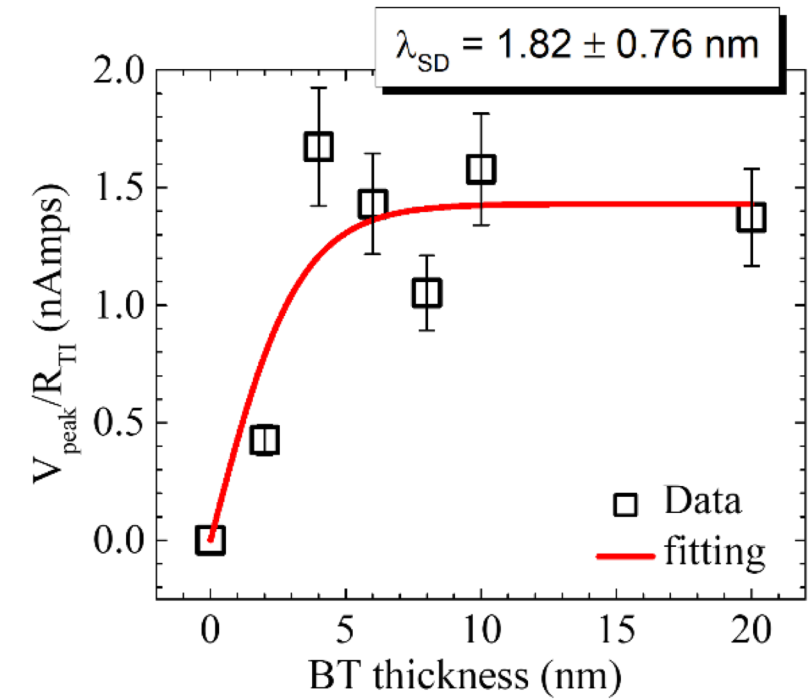
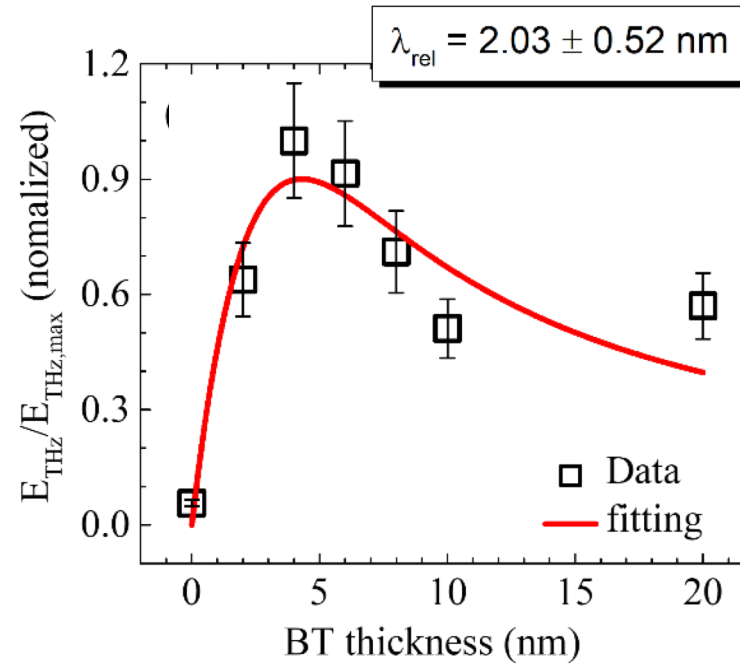
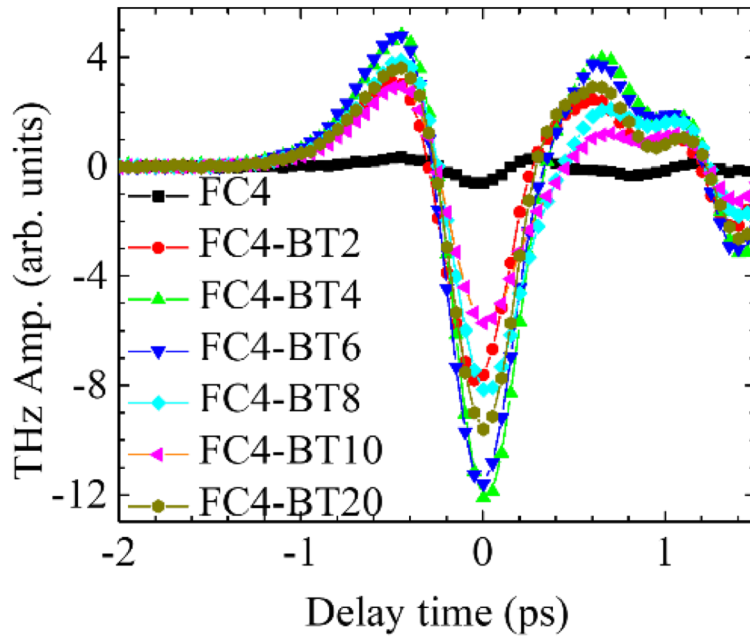
$$\vec{E}_m \sim \hat{n} \times \vec{m} \quad \vec{E}_{ISHE} \sim \frac{\partial J_c}{\partial t} \sim \frac{\partial(\theta_{ISHE} \cdot \vec{J}_S \times \hat{\sigma})}{\partial t}$$

ISHE in Bi₂Te₃



Magnetic dipole radiation

Spin-diffusion length - comparison



Spin diffusion lengths determined from experiments at different time scales in agreement.

Take-home messages - Part 2



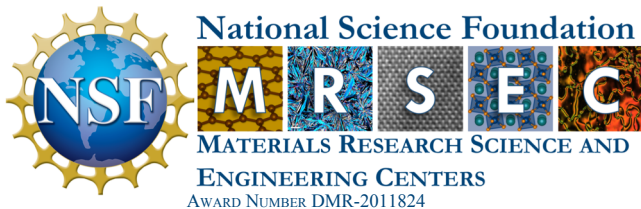
- Observation of spin pumping induced ISHE signal in FeCo/BiTe; additional contribution from high AMR of Fe₇₅Co₂₅ is revealed.
- Extracted spin-diffusion lengths obtained from the two experiments agree well despite the drastically different time scales.
- FMR-induced spin pumping and ultrafast spin-current injection are promising complementary tools to investigate inverse spin Hall effect.

Fe₇₈Ga₁₃B₉/Bi₈₅Sb₁₅ results:

Phys. Rev. Materials **5**, 124410 (2021)

Fe₇₅Co₂₅/Bi₂Te₃ results:

Appl. Phys. Lett. **122**, 072403 (2023)



Recent tutorial article on Principles of THz spintronics:
Wu et al., J. Appl. Phys. **130**, 091101 (2021)